Experiments on seismic behaviour of steel sheathed cold-formed steel shear walls cladded by gypsum and fiber cement boards

Saeed Mohebbi[a], Seyed Rasoul Mirghaderi[a], Farhang Farahbod[b], Alireza Bagheri Sabbagh[c] Shahabeddin Torabian [a,d]

[a] *School of Civil Engineering, College of Engineering, University of Tehran, Tehran, Iran*
[b] *Building and Housing Research Center (BHRC), Tehran, Iran*
[c] *School of Engineering, University of Aberdeen, Aberdeen, AB24 3UE, UK*
[d] *Department of Civil Engineering, Johns Hopkins University, Baltimore, MD*

Abstract

In this paper experiments are presented to investigate the seismic response of steel sheathed cold-formed steel (CFS) shear walls using gypsum and fiber cement board claddings. Six steel sheathed wall specimens of various cladding configurations were tested under cyclic loading. The use of claddings at either or both sides of the walls results in an increase of their lateral stiffness, shear strength and energy dissipation capacity by up to 67, 80 and 76%, respectively. On the use of claddings connected to the CFS walls their effects on the shear strength must be incorporated into the current design specifications for an efficient and safe design.

Keywords: Cold-formed steel, Shear stud-wall, Steel sheathing, Gypsum and fiber cement board cladding, Shear strength, Energy dissipation.

1. Introduction

Steel sheathed cold-formed steel (CFS) shear walls are identified amongst the lateral load resistant systems in ASCE7-10 [1]. AISI S213-07/S1-09 [2] and recently AISI-S240-16 [3,4] and AISI-S400-16 [5,6] present the nominal shear strength of steel sheathed CFS shear walls of 0.457 and 0.686 mm sheathing thicknesses with aspect ratios (i.e. height-to-width ratios) of up to 2:1 and 4:1, respectively. The use of single and double sided steel sheathing on CFS shear walls

increases their shear strength and energy dissipation capacity [7,8]. The state-of-the-art of the steel sheathed CFS shear walls has been extensively reviewed by the authors elsewhere [7]. To protect the structural elements of the walls against fire and for the finishing purposes, claddings of different types are being used, which are commonly assumed as non-structural components in design. While several research have been conducted on the structural effect of claddings on various configurations of CFS shear walls [9-17], lack of research is evident for that of the steel sheathed CFS shear walls. Adham et al. [9] performed six cyclic loading tests on one-sided X-strap-braced, 2.44 m × 2.44 m CFS shear walls, most of which were cladded by 16 mm gypsum board on both sides. Serrette and Ogunfunmi [10] conducted a comparative experimental work on 2.44 m × 2.44 m strap-braced CFS walls with and without gypsum board cladding. Gad et al. [11,12], based on their experimental and numerical work, concluded that the overall stiffness and strength of the cladded strap-braced shear walls were the sum of the contributions from gypsum boards and strap-braces. Moghimi and Ronagh [13] showed improvements in the racking resistance of shear walls and the distortional buckling resistance of studs and chord members when cladded with gypsum boards. Research have also conducted [14-17] on various configurations of sheathing on the walls using oriented strand board (OSB), corrugated steel sheet and gypsum board led to conclusions highlighting their effects on the shear strength of the walls.

The reported increase of the shear strength of the walls due to the cladding engagement imposes additional forces on the members in the load path towards the foundation. This effect could eventually change the type of failure of the wall elements from a ductile failure (e.g. in sheathing-to-wall fasteners) to a brittle failure (e.g. chord stud buckling). This is particularly important when considering a significant reduction in the energy dissipation capacity of the steel sheathed shear walls caused by the latter failure as recently reported by the authors [7].

Further, shortage of design specification [2-6] on the structural effects of claddings limits the efficient design of such structures. American Iron and Steel Institute (AISI) Lateral Design standard [2] recommends a 30% increase of shear strength when using a wooden sheathing (or OSB) on one side and a fully blocked gypsum board on the other side of the walls subject to wind and other in-plane loading. Summation of the shear strengths of different sheathing material at both sides of the walls is not permitted [2].

A comparative experimental work was conducted at the Building and Housing Research Centre (BHRC) of Iran to study the structural effects (including lateral stiffness, shear strength, ductility and energy dissipation capacity) of cladding on the steel sheathed shear walls. Six full-scale wall specimens using different cladding configurations of gypsum and fiber cement boards were tested under lateral cyclic loading, the results from which are presented in the following sections. The experimental results are compared against the predictions of the most recent standards for estimating lateral strength of walls with multiple layers of the sheathing material and potentials for design improvements are discussed.

2. Testing arrangements

Presented in Table 1 and Fig. 1 are six steel sheathed shear-wall specimens cladded with various gypsum and fiber cement boards configurations. For ease of referencing S, G and C stand for steel sheathing, gypsum and cement boards, respectively. The nominal thicknesses of the steel sheathing and the wall members were 0.5 mm and 1.25 mm, respectively. The gypsum and fiber cement boards were 15 mm and 10 mm thick, respectively. The specimen details, design considerations, test setup, instrumentation, loading protocol and material properties are presented in the following sub-sections.

Table 1
Shear wall test specimens

Specimen	Front side sheathing/cladding	Back side cladding
S	Steel sheet (S)	-
S-G	Steel sheet (S)	Gypsum board (G)
S-C	Steel sheet (S)	Fiber cement board (C)
GS-G	Gypsum board+ Steel sheet (GS)	Gypsum board (G)
CS-G	Fiber cement board+ Steel sheet (CS)	Gypsum board (G)
CS-C	Fiber cement board+ Steel sheet (CS)	Fiber cement board (C)

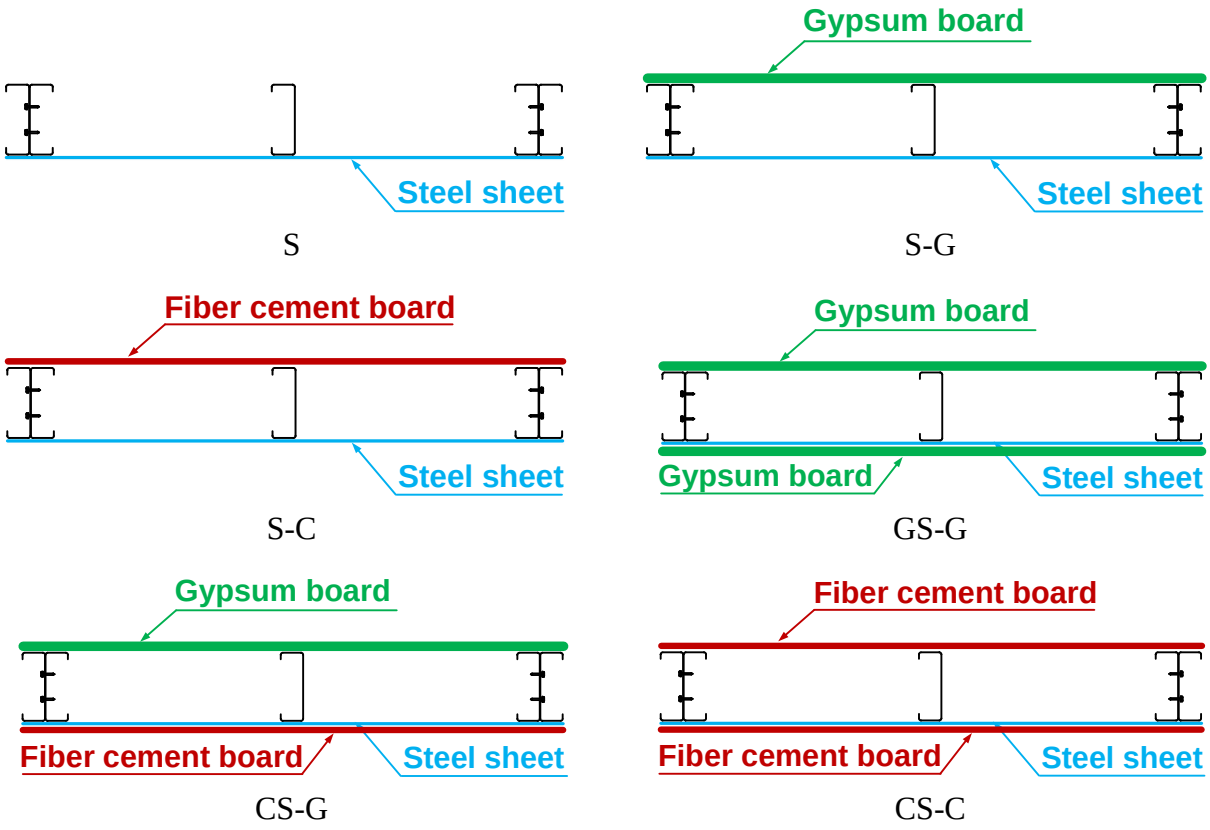

Fig. 1. Plan cross-sections of the specimens

2.1. Specimen details

Fig. 2 shows typical details and screw spacing arrangements of the test specimens. The specimens were 1200 mm wide and 2400 mm high with the studs spaced at 600 m. Built-up

back-to-back lipped channels were used for the chord studs, and a single stud placed in the middle. Single tracks were used at the top and bottom of the walls. The nominal depth of the studs and tracks was 150 mm. The studs were connected to the top and bottom tracks through their flanges by three No. 10×19 mm self-drilling – self-tapping pan head screws. The webs of the built-up studs were connected to each other by two lines of No. 14×32 mm hex washer head (HWH) self-drilling screws at the spacing of 300 mm between the screws in each line. No. 10×19 mm self-drilling – self-tapping pan head screws were used to connect the steel sheathing to the wall frame. The screws were positioned along a single line on the tracks and in a staggered pattern on the chord studs spaced at 50 mm. No. 6×32 mm and No. 8×41 mm self-drilling screws spaced at 200 mm connected gypsum and fiber cement boards, respectively.

Blocking members were placed at the mid-height of the walls, with the same section as the tracks, connected to the interior and chord studs (as seen in Fig. 3). The specific blocking connection detailed to provide higher degree of torsional restraining effect to the studs.

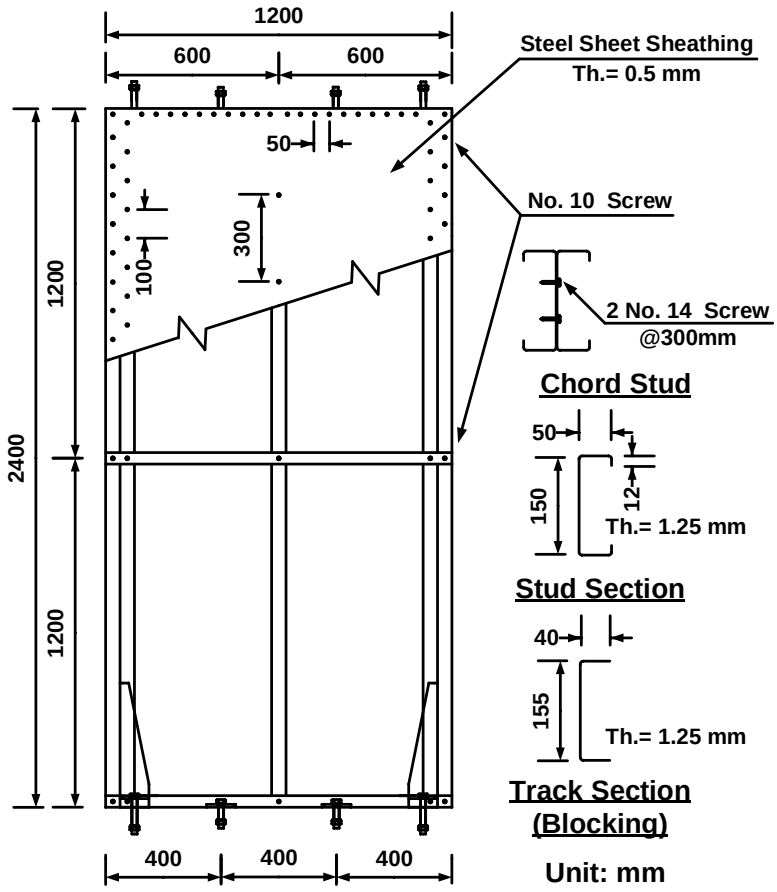

Fig. 2. Framing details and screw arrangement of the test specimens

To resist shear forces four ASTM A325-M16 (with 16 mm-diameter bolts, two at each side) were used to connect the bottom track to the base beam. Two hold-downs (fabricated in the testing lab) connected the chord studs to the base beam via ASTM A490-M20 bolts (20 mm diameter) to resist the overturning forces. Fig. 4 shows the hold-down details and dimensions with relatively thick plates to avoid uplift deformations. Each hold-down was connected to the chord stud through three lines of No. 14×32 mm hex washer head (HWH) self-drilling screws at 40 mm intervals.

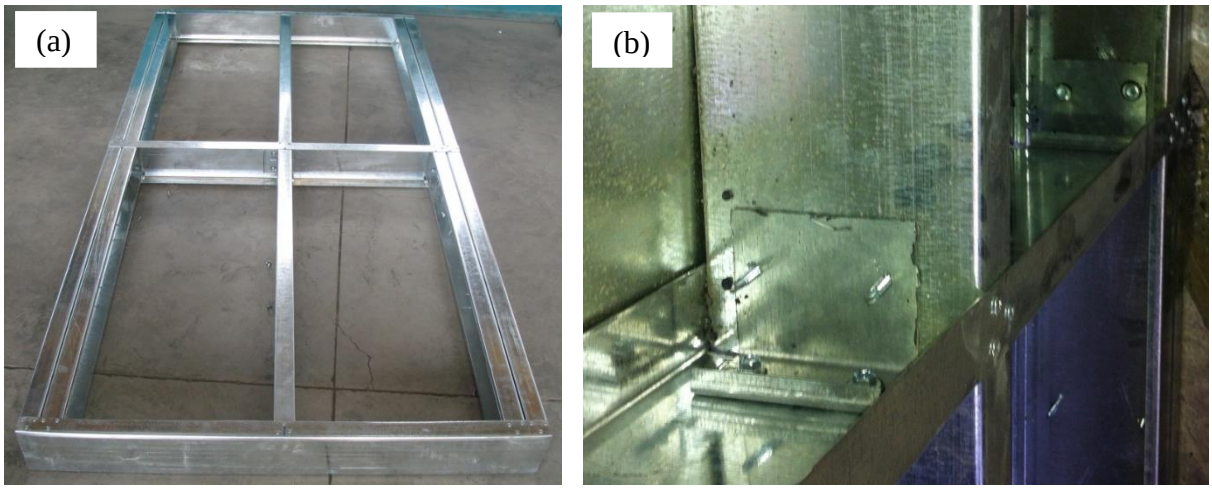

Fig. 3. Blocking details: (a) Frame prior to installation of sheathing, (b) Blocking connection to interior stud and chord stud

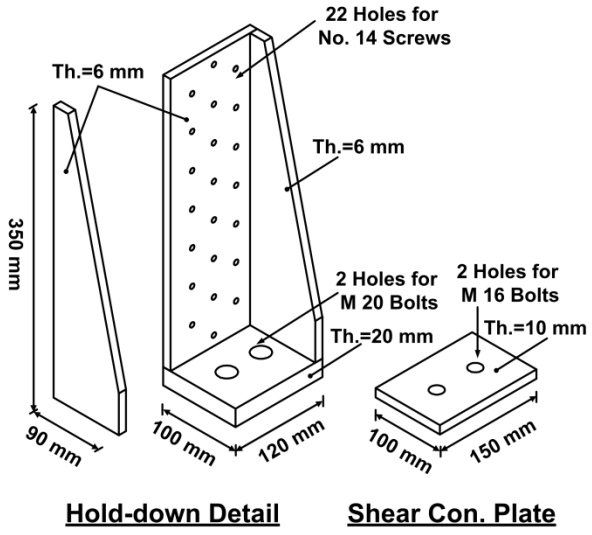

Fig. 4. Details of the hold-down

2.2. Design considerations

To estimate the shear resistance of Specimen S a simplified nonlinear push-over analysis employed as detailed in a related work recently reported by the authors [7]. The steel sheathing was modelled by a number of pin-ended, tension-only diagonal strips. A tension plastic hinge was used at the mid-length of the strips. This accounts for the sum of nominal shear resistance values of the screws attaching the steel sheathing to the wall members [7]. To design the wall

members of the specimens with claddings, 30% and 60% increase to Specimen S shear resistance was assumed for single and double sided claddings, respectively. This assumption is based on recommendations drawn by research conducted on CFS shear walls cladded by gypsum boards [10-17]. The design of the wall specimens was based on the lateral load resistance as the gravity loading would have no detrimental effect when the capacity based approach followed in design [18]**.** Based on the results obtained from the pushover analysis for the steel sheathed specimens and the adopted shear resistance increase for the cladded specimens (mentioned earlier), a capacity design approach was followed for detailed design. An over-strength factor of 1.1 employed to anticipate the demand on the wall elements such as chord studs, hold downs, and shear bolts. Accordingly, the design of the chord studs was governed by the overall buckling and local buckling modes of failure and the hold-downs were designed for the nominal tensile strength of the chord studs.

2.3. Test setup and Instrumentation

Fig. 5 illustrates the wall specimens within the test rig supported on a strong concrete floor, two 500 kN, ±300 mm stroke hydraulic actuators and the instrumentation layout. The top and bottom tracks of the wall specimens were bolted to an auxiliary loading beam and a base beam, respectively. Lateral supports placed at both sides of the loading beam to avoid potential out-of-plane deformations during the tests. The specimens were loaded using a displacement control loading protocol presented in section 3.4. The applied force and the relevant displacements were measured throughout the test. Two universal load cells were placed between the hydraulic actuator and the supporting frames. To measure the vertical and horizontal displacements of the chord and interior studs LVDTs were placed at top, middle and bottom of the specimen (as seen

in Fig. 5). Two strain gauges were pasted on the web of the right chord stud at 1/6 and 5/6 of the wall heights.

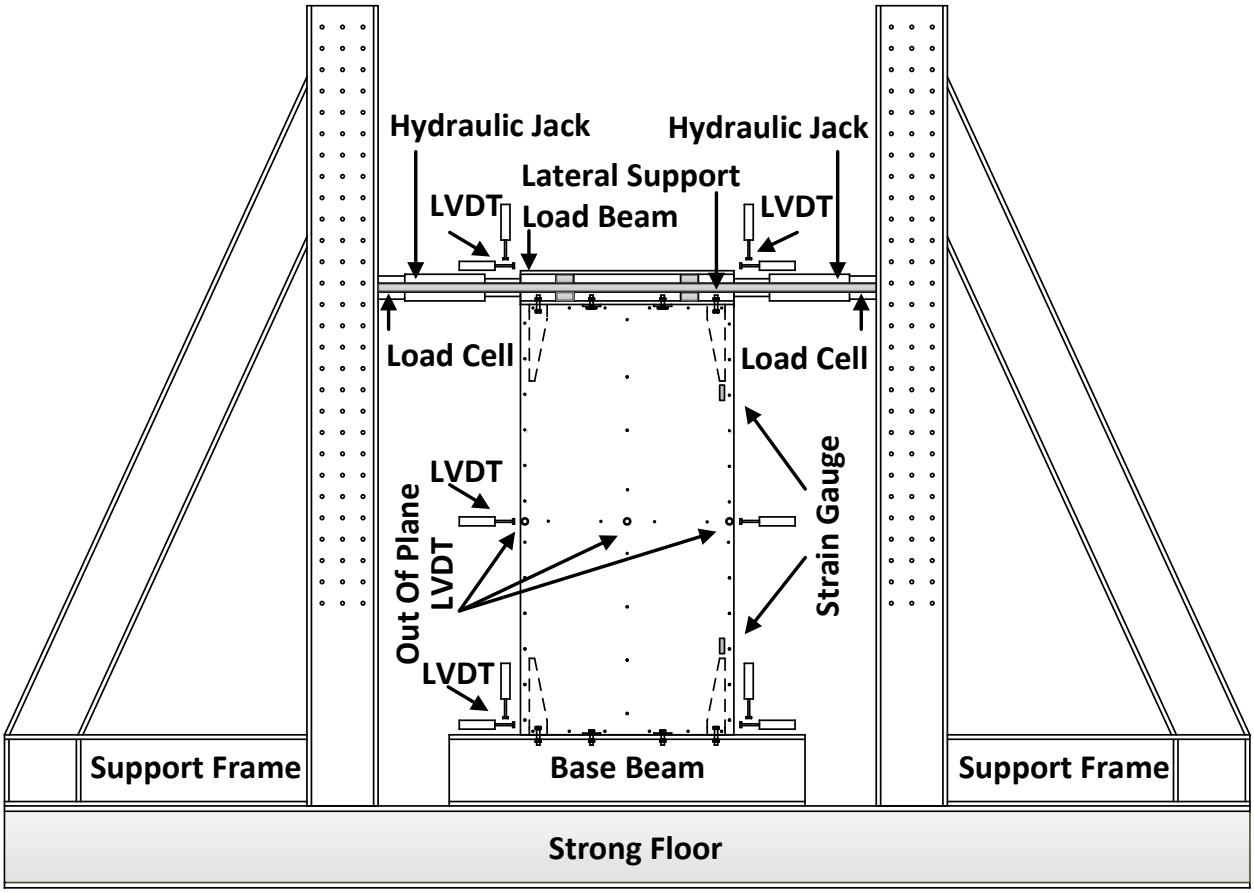

Fig. 5. Test setup and instrumentation layout

2.4. Loading protocol and material properties

Presented in Fig. 6 are the loading cycles applied in conformance with the CUREE protocol specified by Method C in ASTM E2126 [19] in a displacement control mode. The reference deformation, Δ=48 mm (2.0% of the walls height) was used, for consistency purposes, for all specimens.

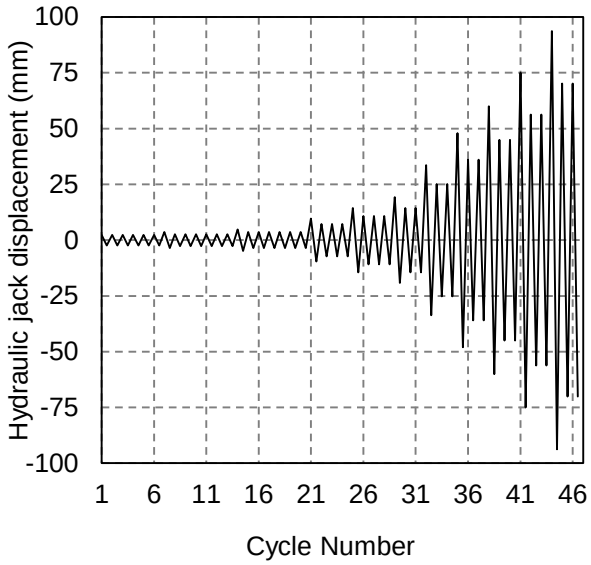

Fig. 6. Loading cycles (CUREE protocol) [19]

Summarized in Table 2 are the stress-strain characteristics of the steel plates obtained via tensile coupon tests conforming to ASTM A370 [20]. The steel grade of 230 MPa, ASTM A1003 [21], was used for sheathing and framing members with the specified minimum yield strength and tensile strength of 230 and 310 MPa, respectively. The zinc coating was removed to measure the true thickness of the tensile coupons. The material ductility specifications of tensile/yield strength greater than 1.08 and the minimum 10% elongation on a 50 mm gauge length required by AISI S100-12 [22] were met.

Table 2
Coupon test results

Member	Uncoated thickness (mm)	Yield strength F_y (Mpa)	Tensile strength F_u (Mpa)	F_u/F_y	Elongation (%)
0.5 mm steel sheet	0.48	273	351	1.29	27
1.25 mm stud/track	1.20	325	356	1.10	34

3. Test results and discussion

The hysteretic behaviour, failure observations, fundamental characteristics, energy dissipation evaluation, strain gauge results and shear strength of the claddings are presented as follows.

3.1. Hysteretic behavior and failure observations

The obtained hysteretic responses and the observed failure modes at different stages of loading of all the specimens are presented in Figs. 7 to 10. The drifts were worked out from the measured displacement at the tip of the walls divided by the total height which is 2400 mm. The points identified by circles on the hysteretic curves represent the observed progressive failure modes described as follows. Points B and B- correspond to the sheathing shear buckling at the early stages of loading. The load sustained and increased in the BC region mainly due to the tension-field action and post-buckling strength in the steel sheathing as well as in-plane shear strength of the cladding. The hysteretic curves show a significant pinching mainly due to the buckling of the steel sheathing during the early cycles. As expected, the peak load (Points C and C-) and the initial stiffness of the walls having claddings on both sides (GS-G, CS-G and CS-C) were higher than those of the walls having one-sided or no claddings (S, C-S and G-S). At the proximity of Points C and C- the steel sheathing fasteners failed in bearing and cracks initiated in the gypsum and fiber cement boards close to their fasteners. These were intensified and caused a sharp strength degradation in CD region. Fig. 8 shows the overall view of the front side (refer to Table 1 and Fig. 1) of all the specimens at 2.5% drift and selective views representing the failures experienced in CD region. A detailed failure observations is described below.

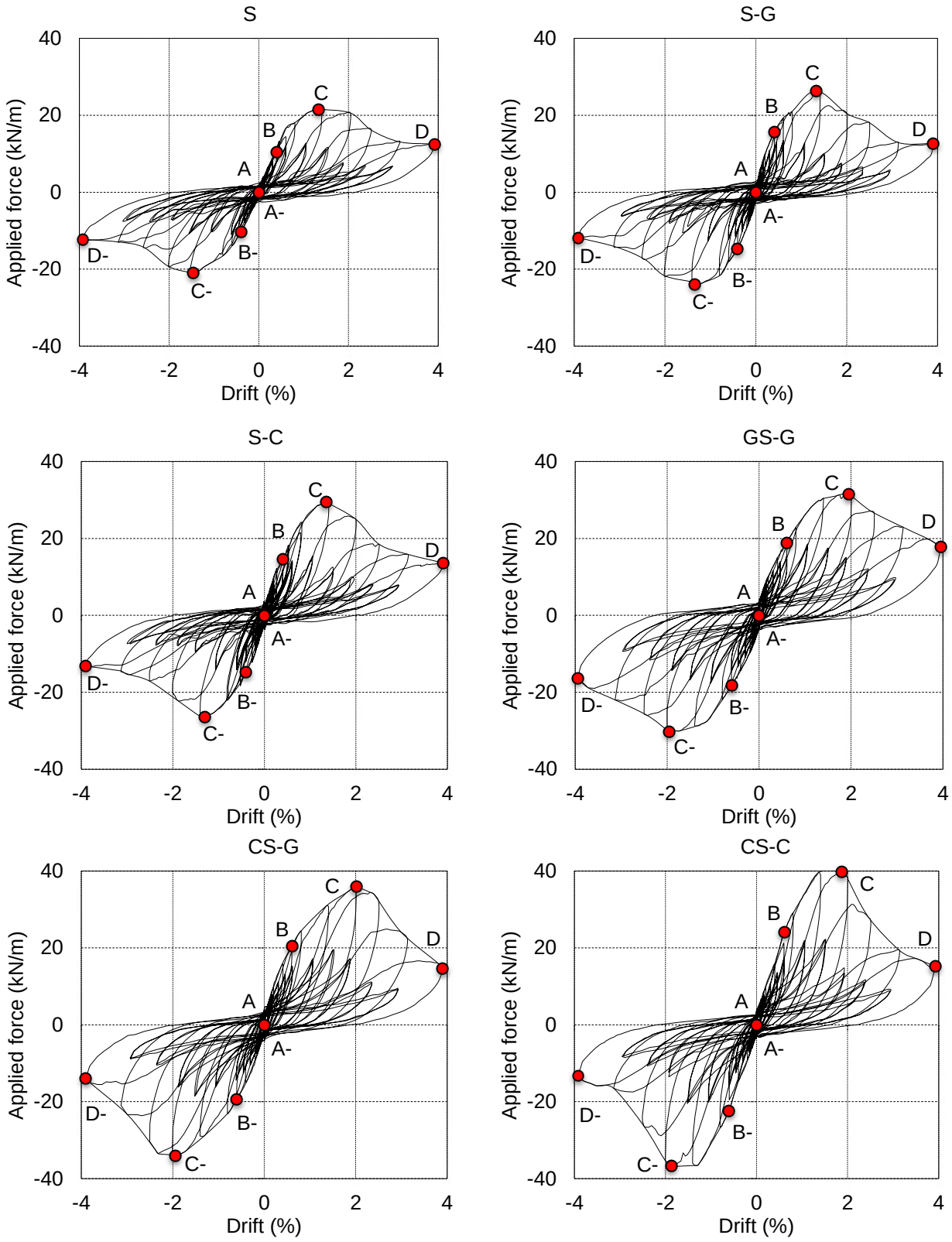

Fig. 7. Experimental hysteresis and envelope curves

Overall views of the front side of all the specimens at 2.5% drift

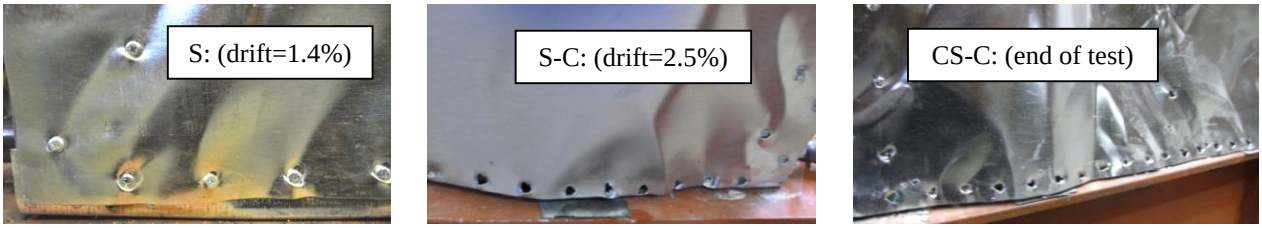

a. Bearing, tilting and pull-through failure in steel sheathing connections

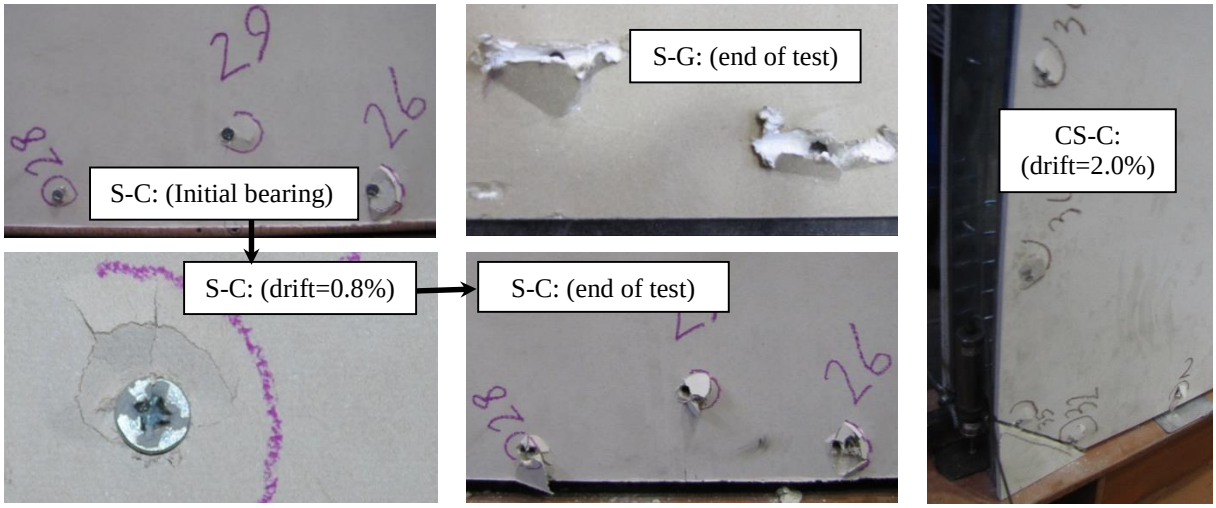

b. Bearing and cracks in cladding connections

Fig. 8. Overall views of the front side of all the specimens at 2.5% drift and selective failure views in the region CD

a. *Bearing, tilting and pull-through failure in steel sheathing connections*

The bearing failure in steel sheathing screw connections intensified by tilting and pull-through modes of failure in higher load increments and finally led to rupture and significant damage around the screw holes. The latter failure is shown for Specimens S, S-C and CS-C selectively in Fig. 8.

b. *Bearing action and cracks in cladding connections*

Bearing action and cracks around the cladding fastener holes occurred mainly due to the non-uniform deformation between the claddings and the wall frames. Buckling and out-of-plane deformation of the steel sheathing caused even more severe damages in these connections. These are shown in Fig. 8 for Specimens S-G, S-C and CS-S (progressively for S-C).

c. *Pulling through failure in claddings*

As seen in Fig. 9, the pulling through failure of the cladding screws at higher loading increments led to partial detachment of the claddings from the wall frames.

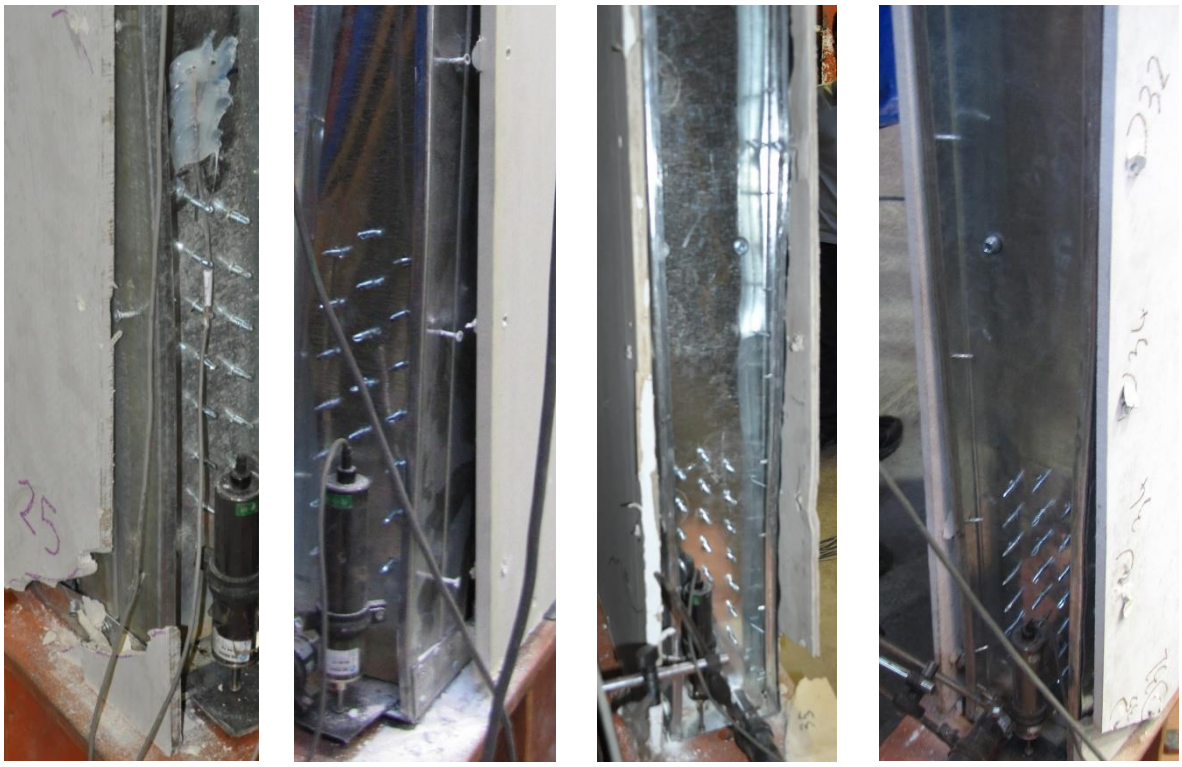

S-C: (drift=3.75%) Back side | S-G: (drift=3.75%) Back side | CS-G: (drift=3.1%) Front side | CS-C: (drift=2.0%) Front side

Fig. 9. Pulling through failure in claddings

d. *Fractures in claddings*

The initiated cracks around the cladding connections caused fractures in the following cycles mainly at the bottom corners where stress concentration developed due to the overturning

moment and the shear force effects. The cladding factures for Specimens S-G and S-C in region CD are shown in Fig. 10.

S-G S-C

Fig. 10. Cladding fractures in region CD

3.2 Fundamental characteristics

Presented in Table 3 are the secant stiffness values at 1% drift, the peak load per length of the walls and the drifts at 80% post-peak load. The use of single and double-sided claddings increased the shear strength by 31 and 80% and the secant stiffness by 32 and 67%, respectively compared to those of the specimen without cladding (Specimen S). These values are those of the specimens having cement board claddings (S-C and CS-C) which were higher than the corresponding values of their counterparts with gypsum board claddings (S-G and GS-G). On comparing the results for different claddings, the CS-C specimen presented more brittle failure in the cladding connections (reported in Section 3.1), thus sharper loss of strength than the GS-G specimen (see Fig. 7).

The drifts at the 80% post-peak load were 2.76, 2.72 and 2.30% for the double sided cladding specimens (GS-G, CS-G and CS-C), respectively. The performance of those cladded by gypsum boards lied within the acceptable limit (greater than 2.5% specified in ASCE7-10 [1]). For the single-sided cladding specimens (S-G and S-C), the obtained drifts were 2.10 and 2.06%, respectively, which are less than the acceptable limit of 2.5%.

Table 3
Fundamental characteristics of the shear walls

Specimen	Stiffness at 1% drift		Peak load		Drift at 80% post-peak load
	(kN/m/mm)	Normalised	(kN/m)	Normalised	%
S	0.80	1.00	21.3	1.00	2.34
S-G	0.95	1.20	25.2	1.18	2.10
S-C	1.05	1.32	27.9	1.31	2.06
GS-G	1.07	1.34	30.9	1.45	2.76
CS-G	1.08	1.36	35.0	1.64	2.72
CS-C	1.33	1.67	38.2	1.80	2.30

3.3. Energy dissipation evaluation

To evaluate the energy dissipation capacity of the cladded shear walls two methods were employed: (i) the equivalent energy elastic plastic (EEEP) curve conforming to ASTM E2126 [19], and (ii) the cumulative energy dissipation. Illustrated in Fig. 11 is the EEEP method; the area under the bilinear elasto-plastic curve equals that of the backbone curve at 80% post-peak load.

The EEEP curve parameters (as seen in Fig. 11) are as follows:

V_{yield} = yielding shear resistance per length of the wall (kN/m)

Δ_{yield} = yielding displacement at V_{yield}

K_e = elastic stiffness per length (kN/m/mm)

Δ_u = displacement at $V_u=0.8V_{peak}$ (post-peak)

A = area under original curve (energy dissipation) at 80% post-peak load

$\mu = \Delta_u / \Delta_{yield}$, the ductility ratio

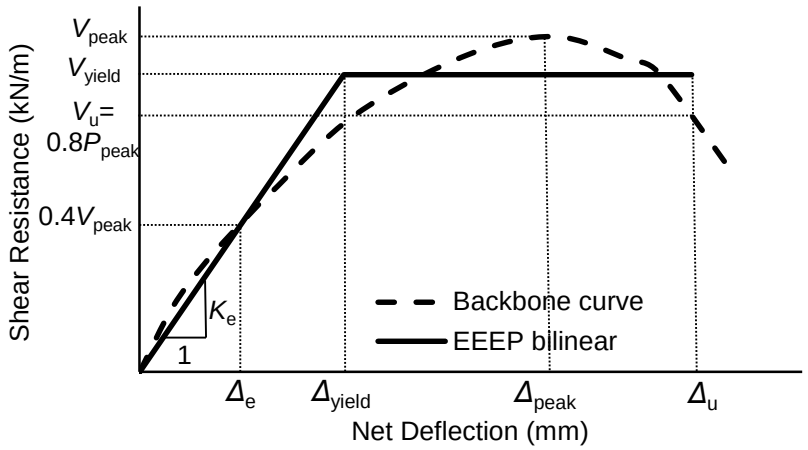

Fig. 11. EEEP Model [19]

Contained in Table 4 are the EEEP results for all the specimens derived from the backbone curves of the hysteretic reversed cycles and the bilinear EEEP curve. The double-sided cladding specimens (GS-G, CS-G and CS-C) dissipated energy in average 60% higher than those with single-sided claddings (S-G and S-C). The highest ductility ratio corresponds to that of Specimen GS-G, which is 27% higher than that of Specimen S with no claddings.

Table 4
EEEP results from reversed cycles

Specimen	V_{yield} kN/m	Δ_{yield} mm	K_e kN/m/mm	V_u kN/m	Δ_u mm	$Drift_{0.8u}$ %	A N.m	μ
S	19.4	17.2	1.13	17.0	56.2	2.34	924	3.3
S-G	21.9	11.4	1.92	20.1	50.5	2.10	979	4.4
S-C	24.2	13.1	1.86	22.3	49.5	2.06	1043	3.8
GS-G	27.2	15.9	1.71	24.7	66.1	2.76	1583	4.2
CS-G	30.3	18.1	1.67	28.0	65.3	2.72	1705	3.6
CS-C	35.8	22.6	1.59	30.6	55.2	2.30	1573	2.4

The cumulative energy dissipation (E) curves derived from the hysteretic load-deformations are shown in Fig. 12. The points marked by symbol “x” correspond to 80% post-peak loads, which

are the intention of comparison herein. The use of double-sided claddings (GS-G, CS-G and CS-C) increased the energy dissipation by 37% and 76% in average compared with that of the single-sided (S-C and S-G) and no cladding (S) specimens, respectively.

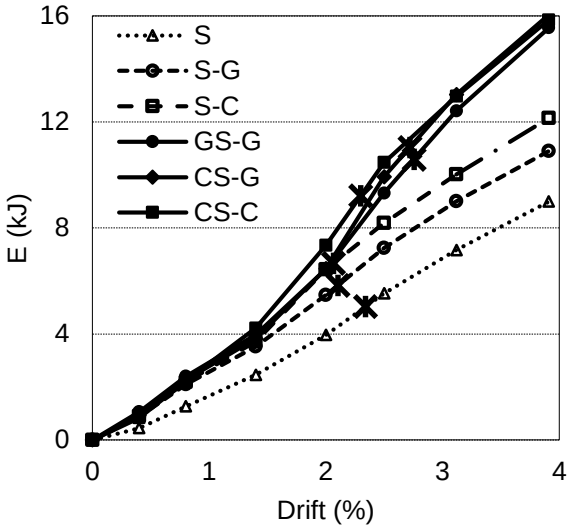

Fig. 12. Cumulative hysteretic energy dissipation of all specimens

3.4. Strain distribution in the chord studs

The strain distribution was recorded along the length of the chord studs (see Fig. 5 for the strain gauges locations), which are the most critical elements of the walls. Fig. 13 (a) shows the strain values normalized to the yielding strain ($\varepsilon/\varepsilon_y$) recorded at the base of the chord studs for Specimens S, S-G and S-C. The maximum strain for each of the specimens, surrounded by a circle in Fig. 13 (a), indicates the magnitudes less than the yielding strain. The strain distribution, however, cannot be assumed uniform over the cross-section due to the local elastic buckling and post-buckling stress redistribution effects. A more acceptable approximation of the chord studs force levels can be obtained by calculating the normalised average stresses shown in Fig. 13 (b). This calculation can be performed setting the external equations of equilibrium of the wall. The higher strain values in the cladded specimens showing an increase up to 68% reflect higher

induced loading demand in their wall elements. This increase must be considered in design to avoid un-favourable modes of failure. Some aspects of design are addressed in Section 4 as follows.

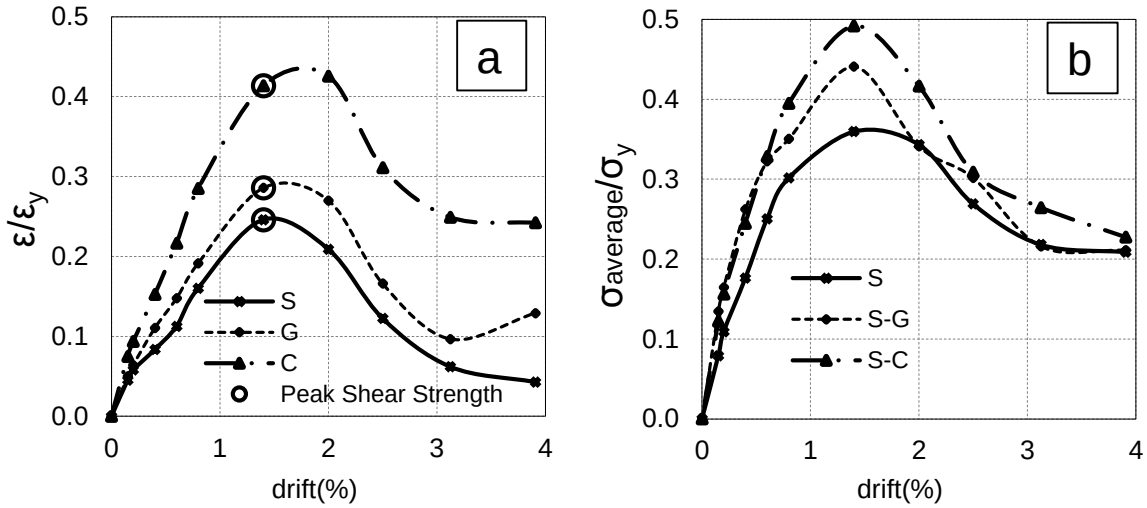

Fig. 13. (a) Normalised local strains (ε_y = 0.2%) at the base of the chord studs, (b) normalised average stresses (σ_y = 230 MPa) for Specimens S, S-G and S-C.

3.5. Shear strength of the claddings

Fig. 14 shows the envelope curves of the tested specimens (dashed lines) subtracted by the base Specimen S (solid line), representing the shear strength of the claddings. It is evident that the effect of the claddings on the wall shear strength is significant (especially for multiple-cladded specimens) and must be accounted for in design as discussed in Section 4.

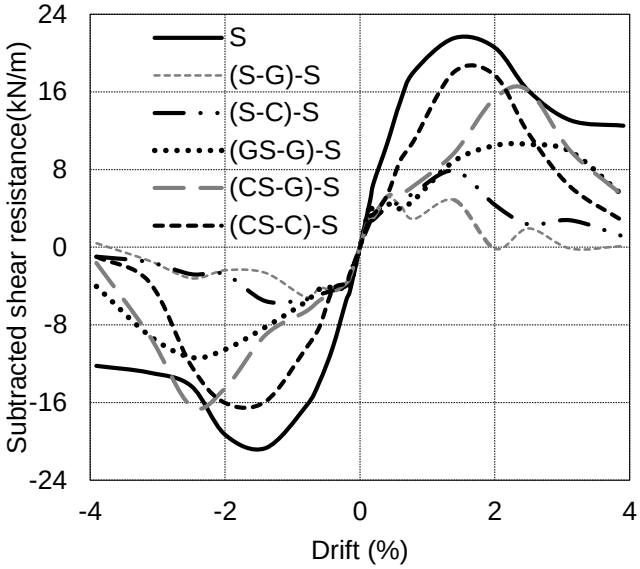

Fig. 14. Subtracted envelop curves of the cladded specimens

4. Design recommendations

The experimental results presented in Section 3.2 showed that cladding steel sheathed shear walls by gypsum and fiber cement boards at either sides would result in a higher shear strength. The design specifications presented in AISI-S213-07/S1-09 [2], however, have not yet incorporated the shear strength increase due to the cladding effects of a variety of materials comprehensively. This is due to the shortage of research on shear walls having different sheathing materials. In the following sub-sections the nominal shear strength of the walls tested in this study are discussed comparatively to the design specifications.

4.1. Nominal shear strength using current design specifications for multiple-cladded walls

Taken into account the current design specifications (AISI-S213-07/S1-09 [2] and recently AISI-S400-16 [5]), for walls with multiple layers of sheathing material, the nominal shear strength (presented in Table 5), $V_{n,\,design}$, can be taken as a greater of two times the shear strength of the weaker ($2\times V_{n,w}$) and the stronger ($V_{n,s}$) claddings. The values for $V_{n,w}$ can be calculated from the

peak loads (V_{peak}) of Specimens S-C and S-G subtracted by that of Specimen S. The shear strength value of 21.3 kN obtained for Specimen S is assumed as $V_{n,s}$ for all the specimens.

4.2. Nominal shear strength based on the overall test results

The nominal shear strength of the tested shear walls also calculated based on the overall test results as presented in Table 5. Two design approaches (specified in US and Canada standards) [2, 6] were adopted based on which the nominal shear strength was calculated as:(i) the smaller value of V_{peak}, the peak shear load and $2.5\times V_{0.5in.}$, the shear value at 0.5 in. displacement (V_{n1}), and (ii) V_{yield} determined by the EEEP analysis (see section 3.3) (V_{n2}). The results show more conservative figures for the latter (V_{n2}). On comparing the available $V_{n,\ design}$ (discussed in Section 4.1) and the adopted approaches in this section the differences are noticeable. The $V_n/\ V_{n,\ design}$ ratios show a maximum of 80% difference between the nominal shear strength based on the overall test results and that of the current specifications which reflect a significant effect of claddings on design which must be taken into account. This is critically important for a safe design using capacity-based design approach in proportioning the wall components. Finally, the over-strength factor presented in Table 5 is the ratio of $V_{peak}/\ V_{yield}$ which can be rounded to 1.10 in design.

Table 5
Nominal shear strength and over-strength values of walls with multiple layers of claddings

Specimens	$V_{n,\ design}$		$V_{n1\ (US)}$		$V_{n2\ (Canada)}$	$V_{n1}/V_{n,\ design}$	$V_{n2}/V_{n,\ design}$	V_{peak}/V_{yield}
	$2\times V_{n,w}$ (kN/m)	$V_{n,s}$ (kN/m)	V_{peak} (kN/m)	$2.5\times V_{0.5in}$ (kN/m)	V_{yield} (kN/m)			
S	-	21.3	21.3	33.6	19.4	1.00	0.91	1.10
S-G	7.80	21.3	25.2	43.5	21.9	1.18	1.03	1.15
S-C	13.2	21.3	27.9	44.2	24.2	1.31	1.14	1.15
GS-G	7.80	21.3	30.9	43.0	27.2	1.45	1.28	1.14
CS-G	7.80	21.3	35.0	45.9	30.3	1.64	1.42	1.16
CS-C	13.2	21.3	38.2	50.8	35.8	1.80	1.68	1.07

5. Concluding remarks

By means of experiments the effect of gypsum and the fiber cement board claddings on the seismic performance of the steel sheathed CFS shear wall structures has been studied. Six specimens were designed and tested under cyclic displacement-control loading. The following conclusions are drawn:

- The shear strength and secant stiffness of the CFS steel sheathed walls can be increased by up to 31 and 32% for single-sided and 80 and 67% for double-sided claddings, respectively.
- The hysteretic energy dissipation can be increased by 37 and 76% in average when using double sided claddings compared to single-sided and walls with no cladding.
- The ductility ratio can be increased when using claddings on either sides provided brittle failures avoided in the cladding connections and thus sharp strength degradation (occurred in specimen with double-sided cement boards) prevented.
- The required 2.5% drift at 80% post-peak load specified by ASCE7-10 was exceeded by the double-sided cladding specimens using gypsum boards at either or both sides.

- Following the capacity based design approach the specifications on the wall shear strength available in the current standards do not suffice efficient and safe design and need to incorporate the effect of variety of cladding materials.

Acknowledgments

The authors are grateful to the Building and Housing Research Center (BHRC) of Iran for providing testing equipment and technical support and Paya Sazeh Pasargad CO, Knauf Iran CO and SHERA CO for providing testing specimens and materials.

References

[1] ASCE/SEI 7. Minimum design loads for buildings and other structures. USA: American Society of Civil Engineers; 2010.

[2] AISI-S213-07/S1-09. North American standard for cold-formed steel framing – Lateral design. Washington, D.C.: American Iron and Steel Institute; 2009.

[3] AISI-S240-16. North American standard for cold-formed steel structural framing. Washington, D.C.: American Iron and Steel Institute; (Final draft passed by the committee).

[4] AISI-S240-16. Commentary on North American standard for cold-formed steel structural framing. Washington, D.C.: American Iron and Steel Institute; (Final draft passed by the committee).

[5] AISI-S400-16. North American Standard for Seismic Design of Cold-Formed Steel Structural Systems. Washington, D.C.: American Iron and Steel Institute; (Final draft passed by the committee).

[6] AISI-S400-16. Commentary on North American Standard for Seismic Design of Cold-Formed Steel Structural Systems. Washington, D.C.: American Iron and Steel Institute; (Final draft passed by the committee).

[7] Mohebbi S, Mirghaderi R, Farahbod F, Bagheri Sabbagh A. Experimental work on single and double-sided steel sheathed cold-formed steel shear walls for seismic actions. Thin-Walled Struct 2015;91:50-62.

[8] DaBreo J, Balh N, Ong-Tone C, Rogers CA. Steel sheathed cold-formed steel framed shear walls subjected to lateral and gravity loading. Thin-Walled Struct 2014;74:232-45.

[9] Adham SA, Avanessian V, Hart GC, Anderson RW, Elmlinger J, Gregory J. Shear wall resistance of lightgauge steel stud wall system. Earthquake Spectra 1990;6(1):1-14.

[10] Serrette R, Ogunfunmi K. Shear resistance of gypsum-sheathed lightgauge steel stud walls. J Struct Eng ASCE 1996;122(4):383-9.

[11] Gad EF, Duffield CF, Hutchinson GL, Mansell DS, Stark G. Lateral performance of cold-formed steel-framed domestic structures. J Eng Struct 1999;21:83-95.

[12] Gad EF, Chandler AM, Duffield CF, Stark G. Lateral behaviour of plasterboard-clad residential steel frames. J Struct Eng ASCE 1999;125(1):32-9.

[13] Moghimi H, Ronagh HR. Performance of light-gauge cold-formed steel strap braced stud walls subjected to cyclic loading. Eng Struct 2009;31:69-83.

[14] Serrette RL, Nguyen H, Hall G. Shear wall values for light weight steel framing. Santa Clara, CA: Santa Clara University; 1996 (Report no. LGSRG-3-96).

[15] Fulop LA, Dubina D. Performance of wall-stud cold-formed shear panels under monotonic and cyclic loading Part I: Experimental research. Thin-Walled Struct 2004;42:321-38.

[16] Xuhong Z, Yu S, Tianhua Z, Yongjian L, Jin D. Study on shear resistance of cold-formed steel stud walls in residential structure. Advances in Engineering Structures, Mechanics & Construction 2006;142: 423-4351.

[17] Liu P, Peterman KD, Schafer BW. Test Report on Cold-Formed Steel Shear Walls. CFS-NEES-RR03, June 2012.

[18] Hikita K, Rogers CA. Combined gravity and lateral loading of light gauge steel frame/wood panel shear walls. Montreal, Canada: Department of Civil Engineering and Applied Mechanics, McGill University; 2006 [research report].

[19] American Society for Testing and Materials (ASTM). Standard test methods for cyclic (reversed) load test for shear resistance of walls for building. ASTM E2126. West Conshohocken, USA. 2007.

[20] American Society for Testing and Materials (ASTM). Standard test methods and definitions for mechanical testing of steel products. ASTM A370. West Conshohocken, USA. 2006.

[21] American Society for Testing and Materials (ASTM). Standard specifications for steel sheet, carbon, metallic- and non-metallic-coated for cold-formed framing members. ASTM A1003/A1003M – 11. West Conshohocken, USA; 2012.

[22] AISI-S100-12. North American Specification for the Design of Cold-Formed Steel Structural Members. Washington, D.C.: American Iron and Steel Institute; 2012.